

SMAST Technical Report 04-05-01

Model Simulations of the Gulf of Maine Response to Storm Forcing**Y. Fan, W. S. Brown, and Z. Yu**

School for Marine Science and Technology
University of Massachusetts Dartmouth
706 S. Rodney French Blvd.
New Bedford, MA. 02744-1221

Abstract

The storm response of the Gulf of Maine/Georges Bank region was investigated using the barotropic version (i.e. uniform density) of the Dartmouth 3-D nonlinear, finite element coastal ocean circulation model with quadratic bottom stress called QUODDY. A suite of model hindcast experiments for the period 4 -18 February 1987 was conducted, in which the model was forced at the open ocean boundaries by the M_2 semidiurnal tidal sea level and in the interior by realistic surface wind stresses featuring a strong 9-11 February nor'easter. Results for a reference model run with a time-space constant drag coefficient C_d of 0.005 captured more than 60% of the observed sea level variance, but left large unexplained model/observed sea level differences, particularly during the storm. Model sensitivity testing to a realistic range of constant C_d values did not improve model results significantly. However, when atmospheric pressure was added to the surface forcing, significant reductions in the model/observed sea level differences were realized.

1. Background

The Gulf of Maine is an inland sea that is separated from the Atlantic Ocean by several shallow offshore banks including Georges Bank (Figure 1). Thus the Gulf responds to wind fluctuations more like an enclosed basin than an open shelf (Brown, 1998). With the exception of occasional hurricanes that pass through the region during summer, the regional wind events in the Gulf are generally much stronger during winter. During the winter stormy season, the Gulf sea level (i.e. barotropic pressure) responds most strongly to near west-east ($255^\circ\text{T}-75^\circ\text{T}$) wind stress fluctuations concentrated in the so-called 2- to 10-day "weather band" (Brown, 1998). The typical westward (eastward) wind stress event during a winter storm of about 1 Pascal (Pa) forces a Gulf-scale average sea level pressure increase (decrease) of about 10 millibars (mbar; or equivalent centimeters). The sea level fluctuations in the western Gulf are about 50% larger than the average. A part of the sea level response is due to the inverted barometric response of Gulf sea level to atmospheric pressure changes associated with the storm. In the deep ocean the inverted barometer response of sea level is almost perfect, thus virtually eliminating direct atmospheric pressure forcing of the ocean (Brown et al., 1975; Wunsch and Stammer, 1997). However, as discussed by Crepon (1976), the inverted barometric response of the coastal ocean is far more imperfect, thus leaving the possibility of atmospheric pressure forcing.

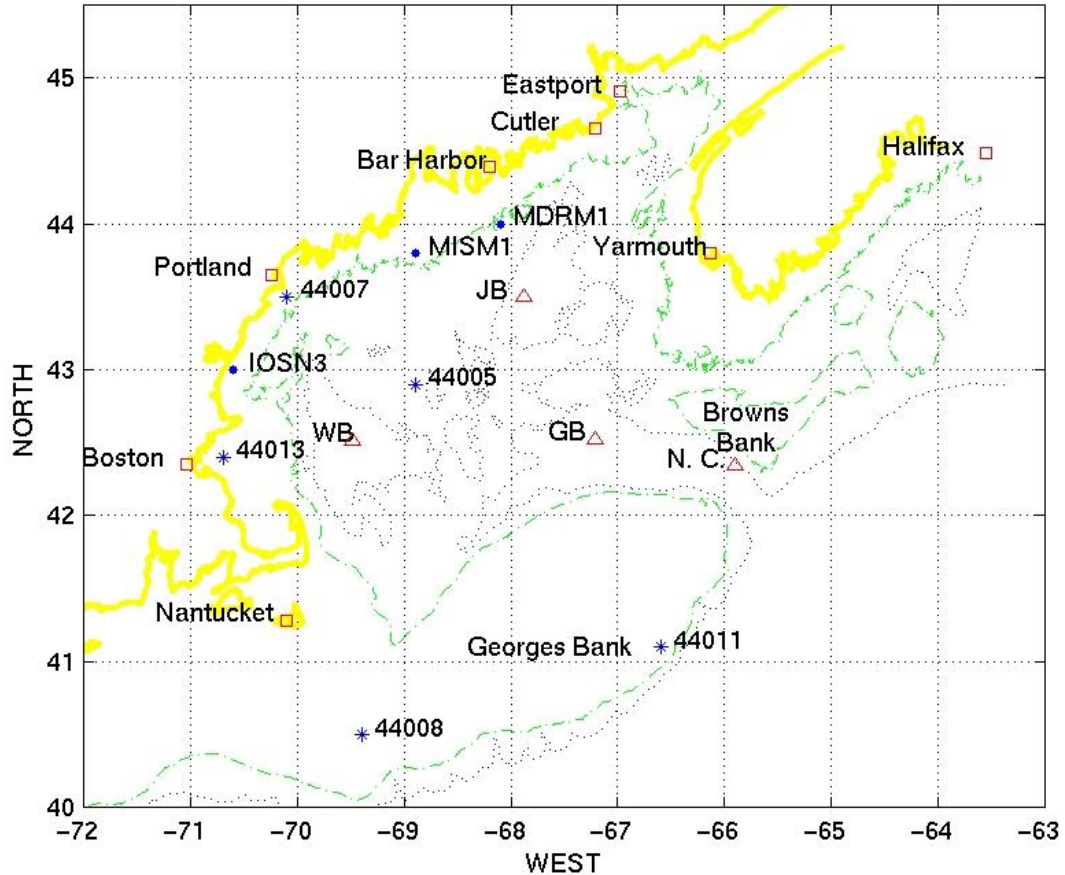


Figure 1. Location map of the Gulf of Maine. The 100m isobath (-.-), and the 200m isobath (....) define the major offshore banks and basins, including Wilkinson (WB), Jordan (JB), and Georges (GB). The NDBC buoys (*) and NWS C-Man (o) meteorological stations, the NOS and MEDS coastal sea level stations (\triangle), and the Brown and Irish (1992) bottom pressure stations (triangle) are also located.

In this paper, we explore the natural storm-induced sea level response of the Gulf of Maine during winter. The approach employs the uniform density (i.e. barotropic) version of the Dartmouth three-dimensional, finite-element circulation model named QUODDY (Lynch et al., 1996; 1997) to simulate the Gulf of Maine response to realistic winds and atmospheric pressure for a study period between 4 and 18 February 1987. The study consists of a series of model hindcasts in which QUODDY was forced with surface wind stress derived from optimally-interpolated winds from an array of National Data Buoy Center (NDBC) buoy and National Weather Service (NWS) C-Man stations (located in Figure 1). In the reference QUODDY run, a space-time constant bottom drag coefficient of 0.005 was used. These model sea level results were evaluated through comparison with the coastal synthetic subsurface pressure (SSP) and observed bottom pressure measurements.

The paper is organized as follows. The QUODDY model is described in section 2. In section 3 we describe the observations and how they are used to force the model. In section 4, the model setup and operations are described. In section 5, the results,

including the effects of including atmospheric pressure, are presented. In section 6, the results are summarized.

2. The Model

QUODDY is a 3-D nonlinear, prognostic, finite element coastal ocean circulation model with advanced turbulence closure (Lynch et al. 1996, 1997). The QUODDY governing equations are expressed in a Cartesian coordinate system on an f-plane as the following Shallow Water Wave Equation (SWWE)

$$\frac{\partial^2 \zeta}{\partial t^2} + \tau_0 \frac{\partial \zeta}{\partial t} + \nabla_{xy} \cdot \left(\tau_0 H \bar{\mathbf{V}} + \mathbf{V} \Big|_{z=\zeta} \frac{\partial \zeta}{\partial t} + \int_{-h}^{\zeta} \left[F_m - \mathbf{V} \cdot \nabla \mathbf{V} + \frac{\sigma}{\rho} (\mathbf{V}_\sigma - \mathbf{V}) \right] dz \right. \\ \left. - gH \nabla_{xy} \zeta - f \times (H \bar{\mathbf{V}}) + H \psi - C_d |\mathbf{V}_b| \mathbf{V}_b + HR \right) = \frac{\partial Q}{\partial t} + \tau_0 Q \quad (1)$$

where ζ is the free surface elevation, τ_0 – a constant, H – total fluid depth ($H = h + \zeta$), $\mathbf{V} = ui + vj$ -horizontal velocity, F_m - non-advective horizontal exchange of momentum, σ – distributed mass source rate, g – gravity, f – Coriolis parameter, $H\psi$ - surface boundary forcing, including wind stress and heat/mass transfer, and $C_d |\mathbf{V}_b| \mathbf{V}_b$ - the quadratic bottom boundary stress. For this application, atmospheric pressure gradient forcing ($-H\nabla P_{\text{air}}/\rho_w$) was implemented (following Young et al., 1995) to QUODDY as an added surface forcing agent. The justification for this is that observations show (see Appendix A) that the inverted barometric sea level response of the coastal Gulf of Maine is imperfect and thus atmospheric pressure forcing should be considered explicitly in dealing with Gulf storm response.

The finite element method is used to solve equation (1). The horizontal model domain is discretized by triangular elements with linear basis functions. The vertical domain is resolved by a terrain-following coordinate system consisting of a string of nodes connected by 1-D linear elements. The governing equations are solved subject to conventional boundary conditions on the horizontal and vertical boundaries. No tangential stress is exerted on the solid vertical surfaces. Elevation, normal flow, or radiation is specified on vertical wet boundaries. At the model ocean surface, specified atmospheric shear stress and or air pressure is imposed; at the bottom a quadratic slip condition is imposed. At the vertical wet boundaries, normal flow from either the post-computed wave equation or a specified quantity is strongly enforced at the boundary in the momentum equations (Lynch et al., 1997). On vertical land boundaries, normal velocity is zero. The kinematic conditions for vertical velocity are specified at the bottom and surface.

3. Observations and Model Forcing Fields

The 4-18 February 1987 study period was chosen because of our comprehensive set of observations that spanned the strong 9-10 February storm. The signature of the storm is clearly seen in the time series records of hourly winds and atmospheric pressures (Figure

2). See [Mupparapu and Brown \(2002\)](#) for more oceanographic details concerning the study period.

Atmospheric Pressure Fields: One challenge was to create reasonably realistic atmospheric pressure (AP) model-forcing fields from the observed data that were not always located optimally relative to the model domain. So, given atmospheric pressure field spatial correlation length scales of hundreds of kilometers, we chose to linearly interpolate the hourly atmospheric pressure measurements to the model mesh elements. However, to implement this strategy, we needed to (1) “relocate” the coastal NDBC/NWS AP stations in the western Gulf to the coast (justified by the very large length scales of the pressure field); AND (2) create several virtual AP stations at several locations along the model open ocean boundary as shown in [Figure 3](#). Specifically this construction required that we assume that (1) the Mount Desert Island (MDRM1) AP record (with a 2-hour delay) was a reasonable approximation to the unavailable Halifax AP; (2) a 2-hour delayed version of the Georges Bank (44011) AP record was a reasonable approximation to the oceanic AP midway along the Halifax cross-shelf transect; (3) a 4-hour delayed version of the Nantucket Shoals (44008) AP record was a reasonable approximation to the oceanic AP at the seaward end of the Halifax cross-shelf transect; (4) the Nantucket Shoals AP record was a reasonable approximation to the oceanic AP at the southwest corner of the model domain. The [Figure 3](#) example shows that this scheme produced a reasonable representation of the AP forcing field associated with the 10 February storm and that most of its impact was concentrated in the parts of the model domain that were seaward of Georges Bank.

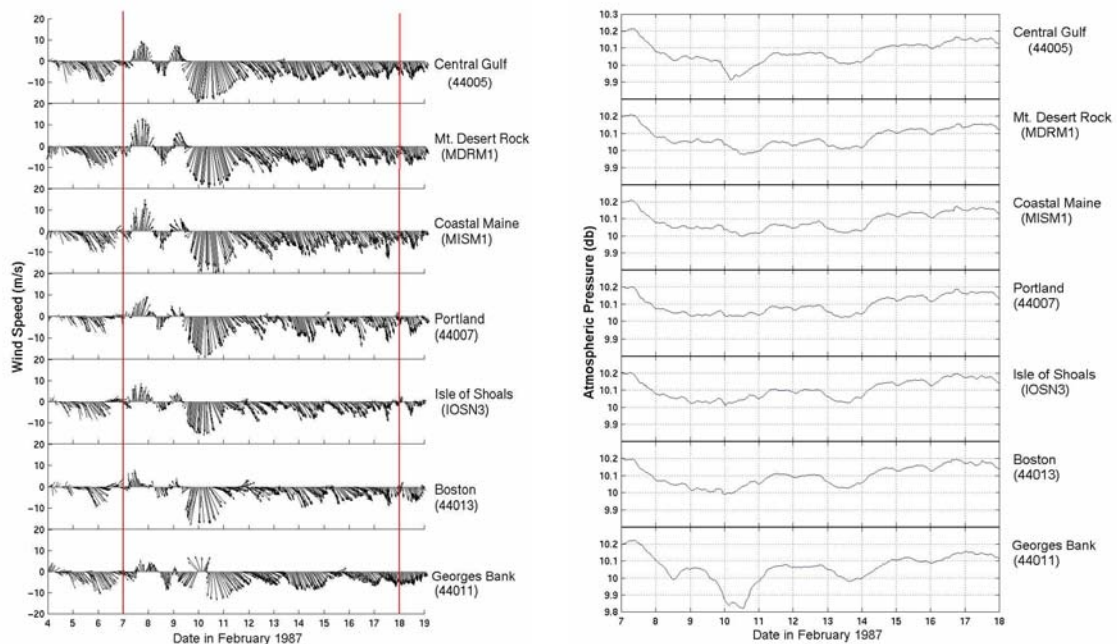


Figure 2. (left) Hourly wind vectors and (right) atmospheric pressures at an array of NDBC buoy and NWS C-Man stations in the Gulf of Maine, the research period is also indicated. See [Figure 1](#) for locations.

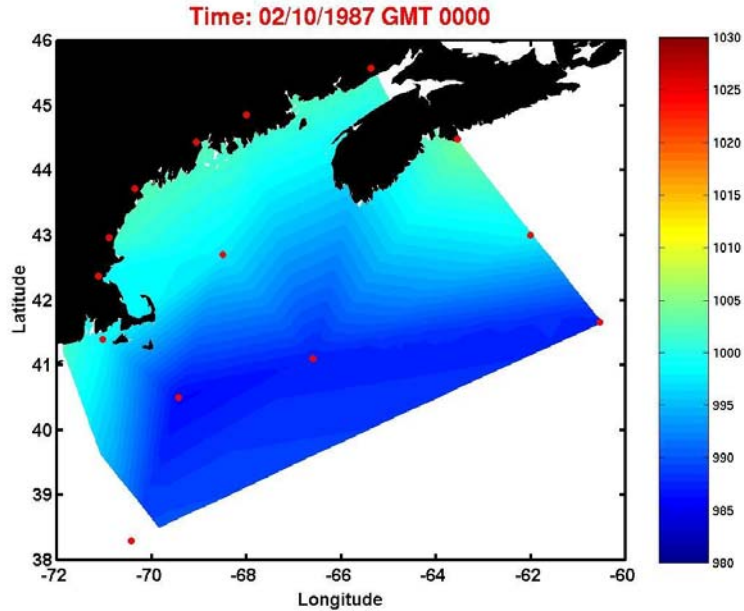


Figure 3. The 0000 UTC 10 February 1987 example of the atmospheric pressure fields (mb scale to the right) that were included in the forcing of some of the QUODDY model runs. These atmospheric pressure fields were derived through linear interpolation (see text) of measured atmospheric pressures at the indicated NDBC/NWS stations.

Model Wind Stress Forcing Fields: The winds were optimally-estimated for all the model mesh nodes using National Data Buoy Center (NDBC) and NWS C-Man station measurements at sites shown in Figure 1 and methods described in Brown et al. (2004). Then buoy wind speeds (U) were adjusted to a 10m reference height and the wind stresses was calculated (Large and Pond, 1981) according to

$$\tau = \rho_{air} C_w U |U| \quad (1)$$

where $\rho_{air} = 1.22 \text{ kg m}^{-3}$ and if $|U| < 11 \text{ m/s}$, then $C_w = 1.2 \times 10^{-3}$; if $11 \text{ m/s} < |U| < 25 \text{ m/s}$ then $C_w = (0.49 + 0.065|U|) \times 10^{-3}$. The example of the wind stress field on the first full day of the northeasterly storm in the Figure 4 shows the expectedly strong winds in the Gulf. However note that because of the lack of NDBC/NWS measurements (see Figure 1) the wind stresses in the northeastern (over the Scotian Shelf) and open ocean parts of the model domain are unreliable.

Hourly coastal sea level records were obtained from NOAA national Ocean Service (NOS) and the Canadian Marine Environmental Data Service (MEDS) for the locations around the Gulf indicated in Figure 1. The sea level record at Halifax was used to force the model (see below) along its open cross-shelf boundary. The Gulf of Maine sea level response was defined by the remaining coastal SL and three bottom pressure (BP; see Brown and Irish, 1993) records. The skill of the model, for different scenarios, was diagnosed by using the model-observation differences.

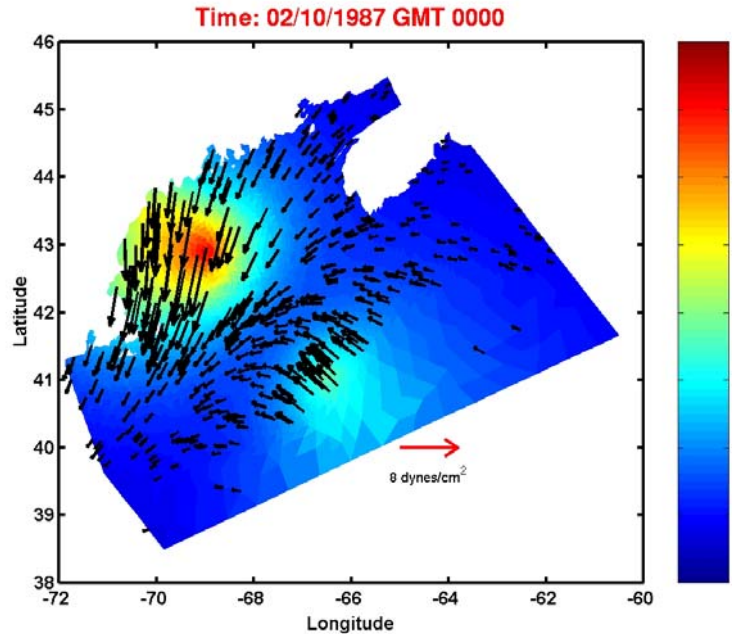


Figure 4. The 0000 UTC 10 February 1987 example of the wind stress fields used to force the QUODDY model.

4. Model Setup and Operations

Model Setup: The QUODDY model domain is defined by the [Holboke \(1998\)](#) GHSD mesh ([Figure 5](#)). The GHSD mesh resolution varies from about 10km in the Gulf to about 5km near the coastlines and even smaller in the regions of steep bathymetric slopes (e.g. north flank Georges Bank). The $(\Delta h)/h_{\min} < 0.5$ condition ([Naimie 1996](#)) is satisfied for mesh elements along the entire shelf break within the domain. A 10m depth minimum was employed the coastal boundary elements. The coastal node of the “upstream” across-shelf open ocean boundary was located at Halifax. It was there that the available MEDS coastal sea level data was used to specify the time-varying sea level boundary condition there.

The model was run in a barotropic mode (i.e. constant density) with steady, homogeneous temperature and salinity fields. The assumed constant temperature of $T = 6.39^{\circ}\text{C}$ and assumed constant salinity of $S = 33.47$ psu were based on the 15m deep moored temperature and salinity, respectively, in Wilkinson Basin for the February 1987 ([Brown and Irish, 1993](#)). The model was initialized with zero velocity and elevation fields.

Model Lateral Boundary Conditions: The conditions imposed along the different QUODDY open boundaries are as follows.

- The Open Ocean Boundary (red line; [Figure 5](#)): The [Lynch et al.\(1997\)](#) predicted semidiurnal M_2 tidal elevation forcing, steady residual elevations (from the initial density fields) and the inhomogeneous, barotropic radiation conditions described by [Holboke \(1998\)](#) were imposed.

- The Southwestern Cross-Shelf Section (red line from Watch Hill, RI; [Figure 5](#)): The [Lynch et al.\(1997\)](#) predicted M_2 tidal elevation forcing, steady residual elevations (derived from the initial density fields) and [Holboke \(1998\)](#) radiation conditions were imposed.
- The Bay of Fundy Section (black line; [Figure 5](#)): The [Lynch et al.\(1997\)](#) predicted M_2 , M_4 , M_6 normal flow constrained by a condition of zero transport across the section were imposed.

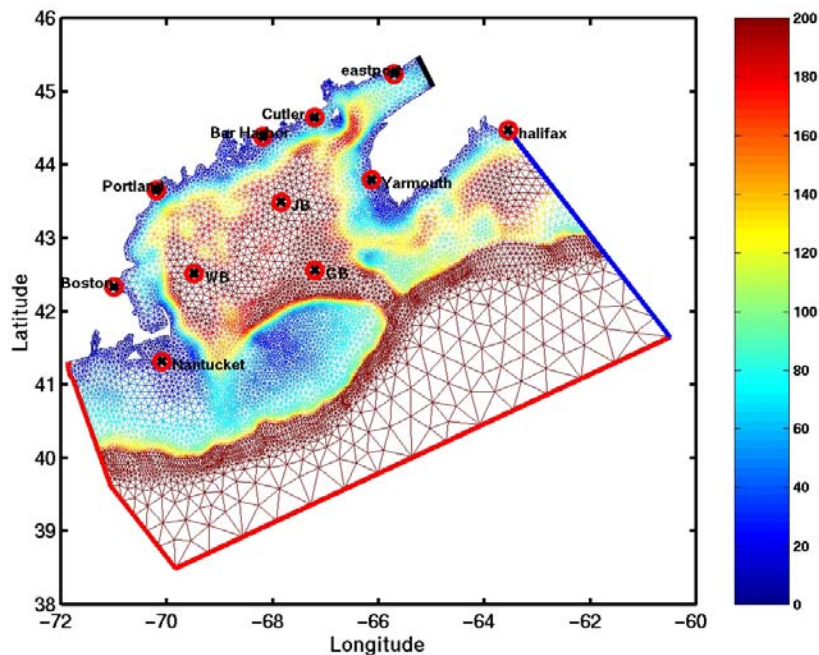


Figure 5. The GHSD mesh for the QUODDY model domain, in which the depth is color-coded (right). The color bar indicates water depth in meters. The sea level and bottom pressure observation stations are located (circled cross) as in [Figure 1](#).

- The Cross-Shelf Section at Halifax (blue line; [Figure 5](#)): The [Lynch et al.\(1997\)](#) predicted M_2 tidal elevation, the [Holboke \(1998\)](#) radiation boundary condition and a “residual” elevation were imposed. The *steady part* of the residual elevation boundary forcing was derived from the initial density fields according to [Naimie et al. \(1996\)](#). An *unsteady part* of the residual elevation boundary forcing was employed to simulate the quasi- arrested topographic wave ([Csanady, 1978](#)) contributions in the form of non-local sea level (i.e. pressure) variability propagating along the Scotian Shelf into the Gulf of Maine. The time-varying Halifax nontidal sea level SL_H was used to drive the [Holboke \(1998\)](#) “smooth-step model” of cross-shelf sea level η_h defined by

$$\eta_h(s) = SL_H \zeta_{nl}$$

in which the normalized cross-shelf structure is given by

$\zeta_{nl} = 1.0 - e^{-(260km-s)/20km}$, with s being the offshore distance from Halifax. As shown in [Figure 6](#), the “smooth-step” sea level extrapolation is nearly constant on

the Scotian Shelf until it reaches the shelf break, where it decreases rapidly. This structure is consistent with the observed behavior of subtidal bottom pressure.

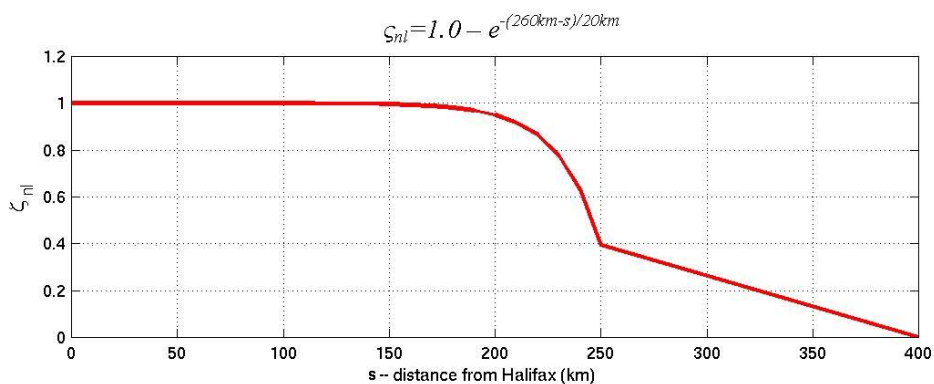


Figure 6. The normalized cross-shelf structure of the smooth-step model of the nontidal (residual) sea level forcing for the Halifax backward cross-shelf boundary.

Model Operations: For each of the experiments, the model simulation was run for 29 M_2 tidal cycles between 2129 UTC 3 February and 2142 UTC 18 February 1987 – dates bracketing the 9-11 February 1987 strong winter storm (see Figure 2). The simulation time step was 21.83203125 sec (= the 12.42hr M_2 tidal period/2048). During the first six M_2 tidal cycles of the model simulation, the tidal amplitude and the wind forcing were increased linearly (i.e. “ramped-up”) so that the model nonlinearities and advection could dynamically adjust the initial fields (Holboke, 1998). Then the model was run with full time-variable forcing for an additional 20 tidal cycles. In the following discussion of the different model experiments that were conducted, differences from the above forcing are explicitly indicated.

5. Results

Like the real ocean, the model response consists of a superposition of three major kinds of contributions from wind forcing. On the largest scale, there is the contribution from remote wind forcing outside of the model domain. Estimates of the contributions due to remote wind forcing are communicated to this model through the “smooth step” model applied to the so-called “backward” cross-shelf boundary at Halifax. Brown (1998) showed that there was remote wind-forced sea level response along the coast in the Gulf of the same order amplitude as that of the Halifax residual sea level fluctuation. On the regional-scale, there is a sea level response due to direct wind-forced Ekman transport in and out of the Gulf (Brown and Irish, 1992; Brown, 1998) as well as gradients in the imperfect inverted barometric response of sea level to atmospheric pressure forcing in the model domain. The combined effects produce a rapid Gulf-scale sea level response via a Gulf-scale Ekman transport. Gulf response on the regional scale is best detected through gulf-scale sea level measurements (Brown and Irish, 1992), which show rapid sea level fluctuations of about 10cm during the winter (i.e. emptying and filling of the gulf). On local scales, there is inertial time-scale sea level and current variability associated with the transients in the adjustment of the larger scale gulf to the regional-scale storm-

forcing. This transient response consists of a cross-isobath sea level warping at the coast (presumably with its associated quasi-geostrophic along-coast flows), that have been observed (Brown and Irish, 1992) to propagate from west to east along the coast. Finally there is the local current and sea level response to local wind forcing. Many of these contributions are aggregated into the sea level results presented below. There is special attention to the currents in a coastal region south of Portland ME.

The *reference QUODDY model run* employed a time/space-constant bottom drag coefficients (C_d) of 0.005 and was forced at the surface by wind stress alone. The model sea level and current results were extracted from an 11-station transect of model mesh nodes between Portland (station 0) and Wilkinson Basin (Figure 7). In what follows the model sea level series are compared with observed sea level records and sea level equivalents of the bottom pressure records in the basins of the Gulf of Maine. The Gulf basin sea levels were inferred from the difference between local atmospheric pressure and measured bottom pressure measurements with the reasonable assumption that there was no significant contribution from water column density-related pressure variability.

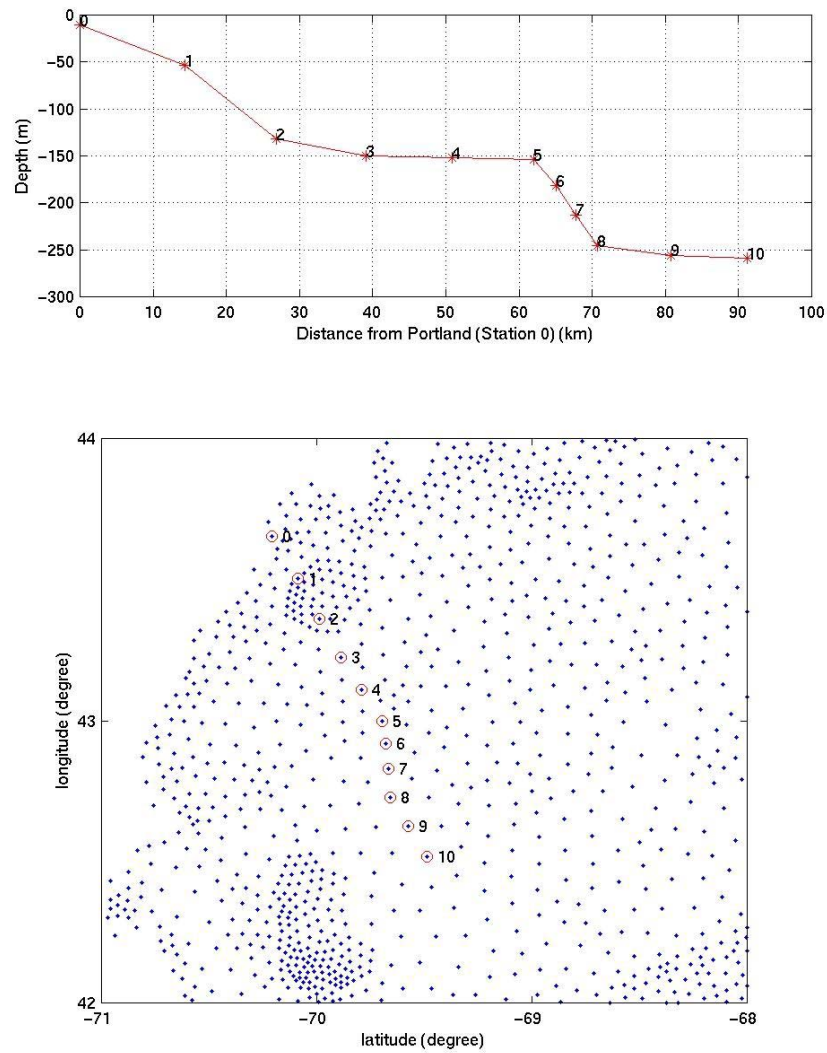


Figure 7. (below) A map of the QUODDY model nodes along the transect between Portland (station 0) and the center Wilkinson Basin (station 10); (above) The transect depth profile.

Though there was some visual evidence of sea level response to the 9-10 February storm winds, the model sea level fluctuations were dominated by the M_2 tidal sea level fluctuation amplitudes that decreased from about 1.1m at Portland (station 0) to about 0.9m at station 10 in Wilkinson Basin. The total sea level fluctuation amplitudes, due to combined tidal and wind stress forcing, decreased from about 1.3m at the coast to about 0.9m in Wilkinson Basin (see [Table 1](#)); the departure from the tidal response hinting at the coastal trapped character of the response to both remote and local wind forcing.

Table 1. Sea level at stations along the Portland/Wilkinson Basin transect (see [Figure 7](#)) for the reference model run.

Station	Equivalent Sea Level Amplitude (m)
0	1.34
1	1.12
2	1.08
3	1.05
4	1.04
5	0.99
6	0.98
7	0.95
8	0.92
9	0.91
10	0.85

By contrast, the model currents near the coast reflect the storm wind forcing against the background tidal variability (see [Figure 8](#)) much more clearly than do the sea level records. The westward storm winds backed to southward over the two duration of this typical strong “nor’easter and produced a robust southwestward currents were coastally intensified, that is stronger at the 50m depth station 1 than at the 125m depth station 2.

Returning to the sea level response and in order to focus on the wind forced sea level response, the predicted tide was subtracted from the model, observed sea level, and sea level equivalent of bottom pressure records (i.e. detided) and then lowpass filtered (cutoff frequency = $(36)^{-1}$ cph) to produce the “subtidal” SL records. The subtidal sea levels for the reference model run in [Figure 9](#) clearly show how the 9 February 1987 onset of northeasterly (i.e. southwestward) storm causes sea levels to rise throughout the gulf. Then, as the winds back to southward on 10 February, the subtidal sea levels throughout the Gulf begin to decrease and continue to do so through 11 February. The model subtidal sea levels show the same general variability as the observed and pressure equivalent sea levels.

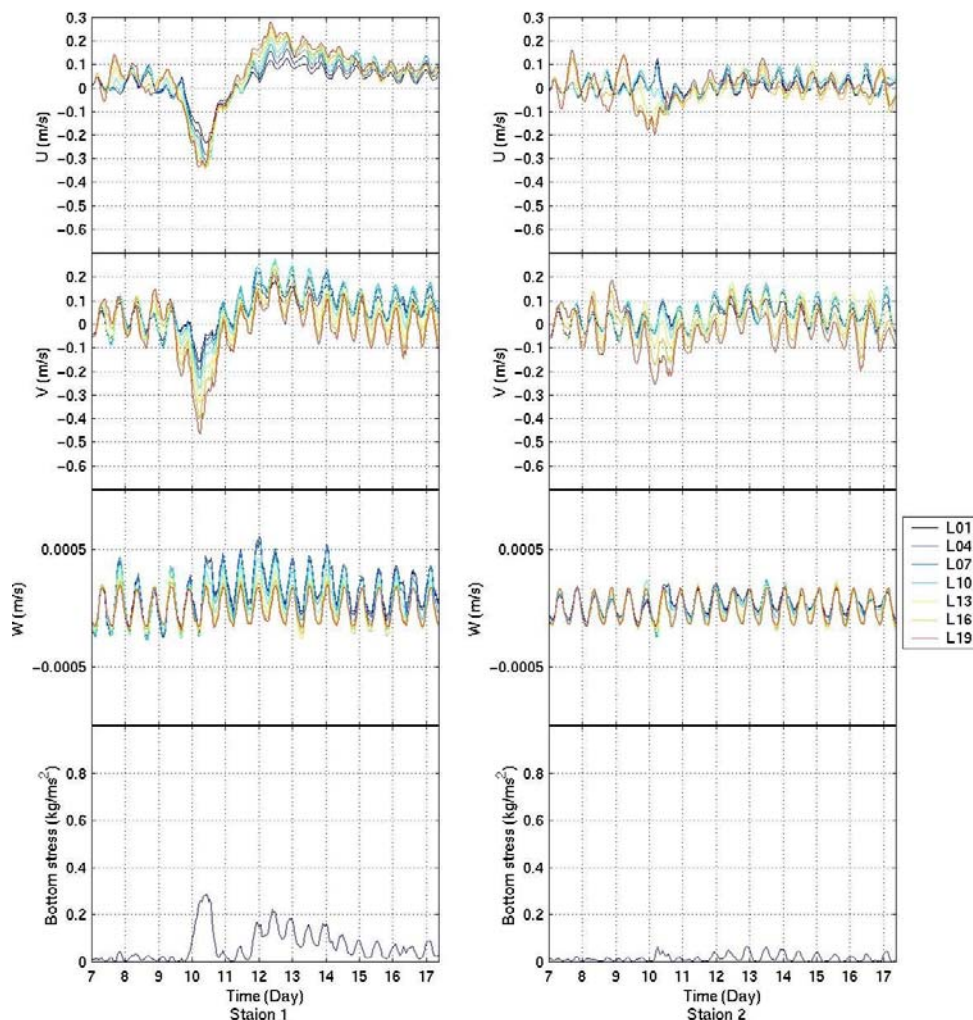


Figure 8. The February 1987 vertical structure of currents at (left) the 50m depth stations 1 and (right) the 125m station 2 for the reference model run ($C_d = 0.005$). The current components in m/s (top 3 panels) eastward U; northward V; upward W at 7 of the 21 model sigma levels (legend on right). (bottom panel) The bottom stress time series.

Quantitatively, this QUODDY model hindcast captures more than 46% of the observed subtidal sea level variance observed at these stations (left 2 columns in Table 2). This result represents a significant improvement over the 31% of the observed variance explained by the Brown (1998) study using the linear FUNDY model simulations. However there still are significant differences between model results and observations, especially during the 9-11 February storm. For examples, (a) the 10 February increase of model sea level is significantly less than the corresponding observed sea level and further (b) its decrease lags that of the observed sea level by a about $\frac{1}{2}$ day.

To address this issue, we tested the sensitivity of the model simulation to choice of C_d values by conducting two other model runs - one with $C_d = 0.0025$ and the other with $C_d = 0.0075$. The amplitudes of the subtidal model sea levels for these different cases are within about $\pm 1.5\%$ of one another (see Table 2). Thus storm-forced model sea levels are insensitive to the values of the drag coefficient even though bottom stress is significant

near the coast (see [Figure 8](#)). Still all of the subtidal model sea level standard deviations are about 30% less than those observed sea levels.

Table 2. The record standard deviations (SD) of the subtidal observed sea levels (in m) are compared with model sea level SDs for cases with $C_d = 0.0025$, 0.0075 , and 0.0050 respectively.

	Observations	$C_d = 0.0050$	$C_d = 0.0025$	$C_d = 0.0075$
Bar Harbor	0.129	0.104	0.106	0.105
Portland	0.157	0.094	0.095	0.094
Yarmouth	0.128	0.087	0.088	0.086
Boston	0.183	0.096	0.096	0.095
Nantucket	0.192	0.106	0.107	0.105
G. B.	0.098	0.075	0.075	0.075
J. B.	0.102	0.080	0.080	0.080
W. B.	0.132	0.089	0.090	0.089
Average	0.140	0.091	0.092	0.091

This insensitivity of the model sea level results to the factor of two differences in C_d is reflected in the [Figure 10](#) presentation of the model skill, as defined by

$$Model \ Skill = 1 - \left(\frac{1}{N} \sum_{i=1}^N \alpha_i \frac{\sigma_{DPi}^2}{\sigma_{OP}^2} \right) ,$$

where N is the number of time series, σ_{DP}^2 is the variance of the model-observed sea level difference time series, σ_{OP}^2 is the observed sea level variance, and the weights $\alpha_i = 1$. Thus we had to look elsewhere to explain the significant discrepancy between model and observed sea levels.

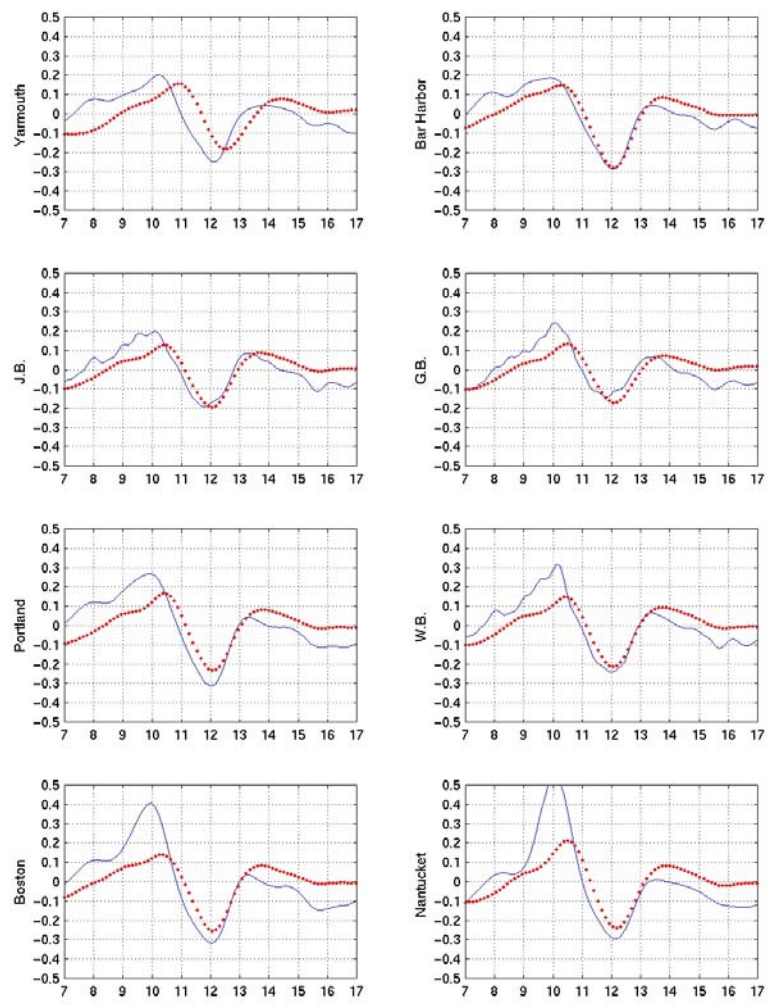


Figure 9. The February 1987 subtidal sea levels from the 0.005 constant C_d QUODDY model simulation and measurements at some of the stations shown in Figure 1; The observed (blue line) and model subtidal sea levels (red dotted line) are presented.

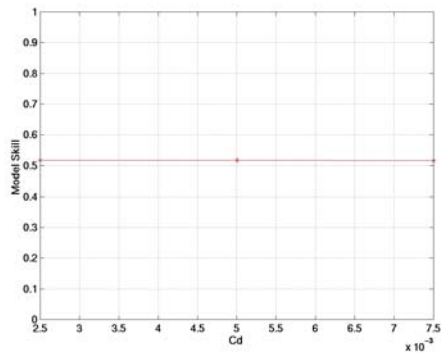


Figure 10. Skill level of the QUODDY model sea levels for different constant C_d values.

We hypothesized that there would be greater model sensitivity to different specifications of the meteorological forcing. To test this hypothesis, atmospheric pressure gradient forcing was added to wind stress forcing in the model (as described in section 2). With this modification, the reference QUODDY run (with $C_d = 0.005$) was run with “observed” atmospheric pressure as described in section 3. The visual comparison between the subtidal model and observed sea levels during the 9-11 February storm (Figure 11) is a clear improvement over that of the reference QUODDY run (in Figure 9).

The excellent matches seen in the eastern gulf at Yarmouth and Bar Harbor are degraded somewhat in the western gulf with slight model under-predictions of the storm forced peak at Portland and Boston. There are also some issues that need to be explained in future work including the “over-prediction” of the post-storm sea level depression in Georges and Jordan Basins. But the quantitative improvement seen in this QUODDY experiment is clear, with a model capture of 82% of the total variance of the observed subtidal sea levels suite. The corresponding improvement of the skill from 0.52 to 0.81 is notable.

Clearly atmospheric pressure forcing needs to be included in the model forcing to achieve first order match with the observed Gulf subtidal storm response. In retrospect however, the conclusion that atmospheric pressure needs to be included in the QUODDY storm response calculation should not be a surprise, given that atmospheric pressure forcing has been an integral component of most storm surge models (e.g. Flather, 1994; Blain et al., 1994) that are being used.

6. Discussion of Results

The barotropic application of the 3D finite element QUODDY model to the Gulf of Maine region has produced a very respectable simulation of the storm of 9-11 February 1987 - based on explaining 82% of the variance of an extensive suite of sea level observations.

But to what do we attribute the other 18% of the observed sea level variance? Surely some of the remaining discrepancy is due to uncertainties in our estimates of: (1) both wind stress and atmospheric pressure forcing; (2) remote wind-forcing at Halifax; (3) tidal effects due to our use of only the M_2 tidal constituent. The model sea level sensitivity to uncertainties in these forcing agents is underway. Then there is the unknown importance role of space-time variable bottom stress due to the effects of the 12s surface gravity waves in water shallower than about 100m.

The vertical structure of the currents at the different transect stations is displayed in the Figure 12 hodographs for stronger and weaker wind forced cases at 0537 UTC and 2242 UTC 10 February 1987 respectively. For the stronger wind case (winds $\sim 20\text{m/s}$; wind stress $\sim 8.4\text{ dyn/cm}^2$), the *surface currents* are directed generally toward the classical 45° to the right of the wind stress, ranging in speed from 0.31m/s at station 10 to 0.56m/s at station 1 (about 2% of the wind speed). However, the structure of these current profiles, looking rather like an incomplete Ekman spiral differs from the classical one. We

speculate that the relatively strong wind forcing causes increased the water column eddy viscosity and hence an Ekman depth scale (Fan and Brown 2003), that is greater than the water depth. For the weaker wind case ($\sim 11\text{m/s}$ and 1.8 dyn/cm^2), the current hodograph shape is more similar to the classical Ekman spiral. However, the surface current direction is less classical in that it ranges from 20° to 67° to the right of the wind stress at the different stations. Perhaps a more spatially variable near-surface eddy viscosity explains the latter result.

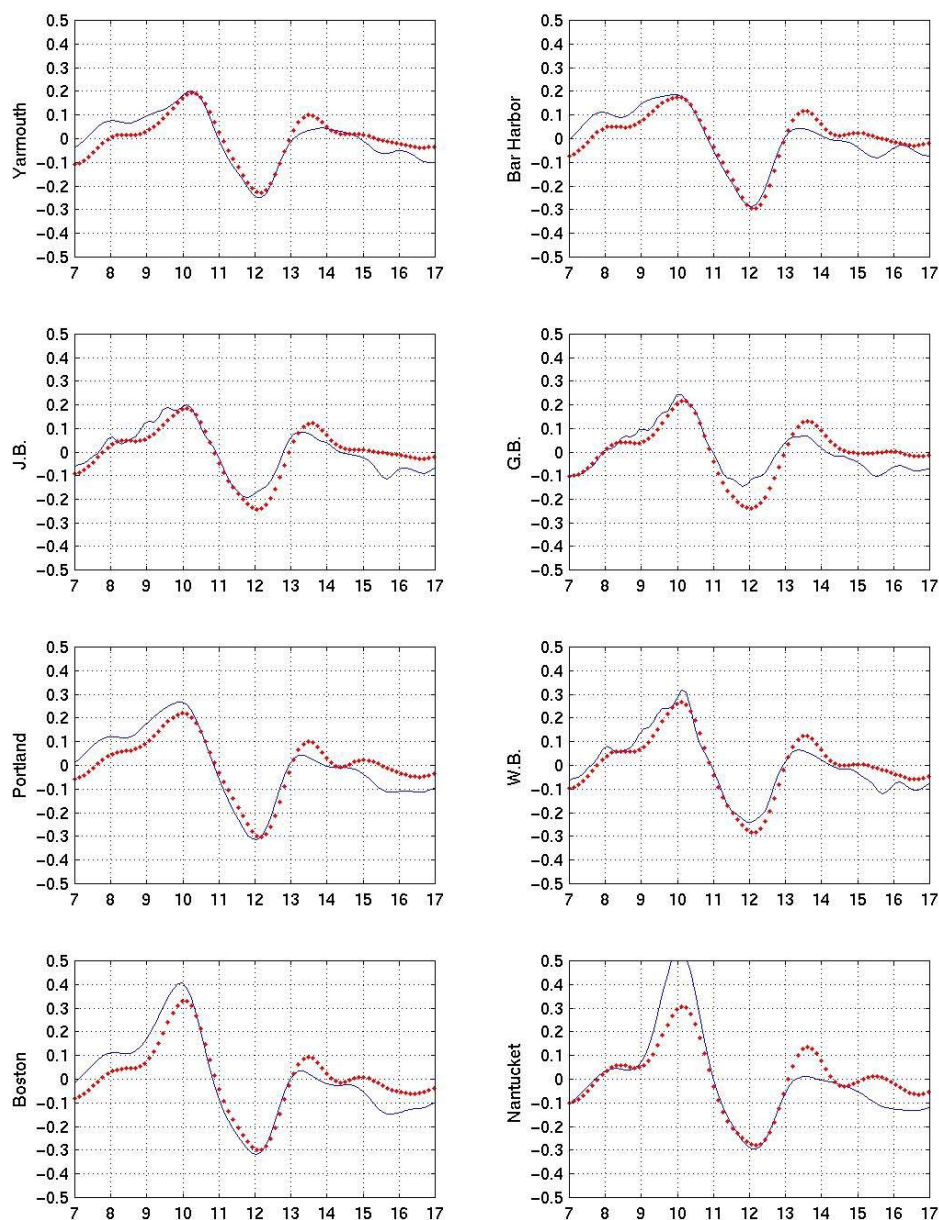


Figure 11. (upper two panels) February 1987 atmospheric pressure at Portland and Boston; (lower two panels) Comparison of wind/pressure-forced (constant $C_d = 0.005$) QUODDY model residual sea level (dotted line) and observed residual sea levels (blank line) at Portland and Boston respectively.

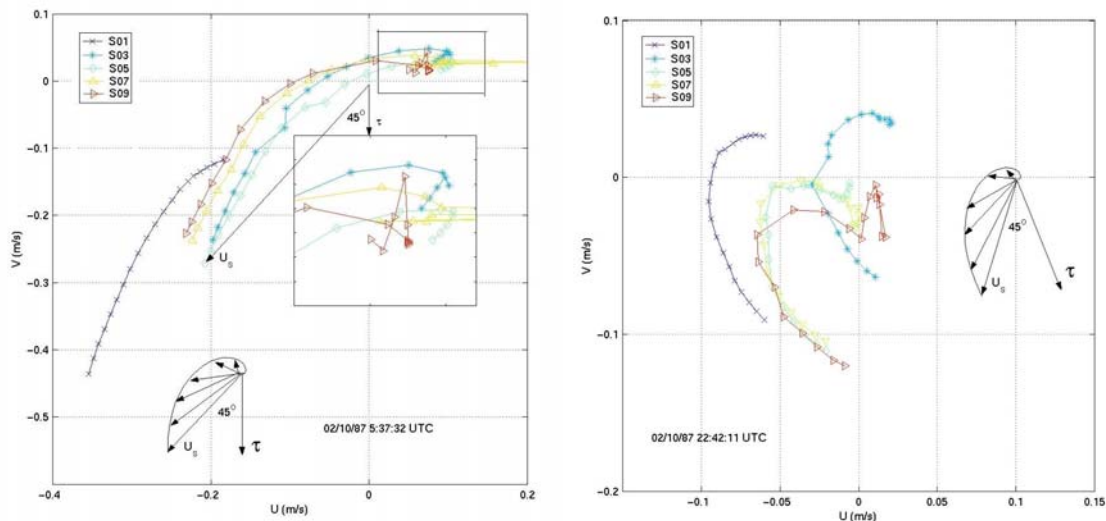


Figure 12. Subtidal model current hodographs at the different transect stations for 10 February 1987 at (left) 0537 UTC with a transect-averaged wind stress magnitude of 8.7 dyn/cm^2 ; and (right) 2242 UTC with a transect-averaged wind stress magnitude of 1.8 dyn/cm^2 . A “classical” Ekman layer hodograph, with the wind stress aligned with the actual wind stress, is shown for reference.

In one set of model experiments runs with the same wind-forcing, QUODDY was coupled with the [Styles and Glenn \(2000\)](#) bottom boundary layer model (BBLM) to simulate space-time variable bottom stress. BBLM used QUODDY-produced bottom currents with NDBC buoy-derived surface waves to produce time-space variable bottom stress that was iteratively fed back into the QUODDY calculation. However the results were inconclusive, probably compromised by inadequate wave data. A focused study of this process and sensitivity to the details of the atmospheric forcing is planned for the future.

7. Summary of Results and Conclusions

In summary, the barotropic QUODDY model, with a space-time constant bottom drag coefficient $C_d = 0.005$ and forced by *only* optimally-interpolated observed wind stress fields, captured 46% of the total variance of the observed subtidal sea levels at 7 coastal and 3 basin station within the Gulf. This result was a significant improvement over the 31% of the variance captured by a comparable calculation using the linear harmonic model FUNDY ([Brown, 1998](#)). The addition of atmospheric pressure gradient forcing to the wind stress-forced reference QUODDY run provided another dramatic reduction in the model/observation sea level differences to the extent that 82% of the subtidal sea level variance was captured on a Gulf scale.

Future work includes using improved atmospheric forcing (winds and pressures) using atmospheric model fields like those provided by the US Navy Fleet Numerical Meteorological and Oceanographic Center (FNMOC). We also expect additional

improvements will come from a coupled BBLM and more detailed specification of the surface waves in the whole Gulf of Maine.

8. Appendices

Appendix A. Inverted Barometric Response in the Gulf of Maine

A visual inspection of in [Figure A1](#) showing the detided Boston and Portland atmospheric pressure (AP) and the pressure equivalent of sea level (SL) records from 7-19 February 1987 clearly reveals a qualitative inverse relation. The cross-correlation functions between AP and SL in both locations [Figure A1](#) confirm these visual conclusions. This tendency for oceanic SL to respond inversely to AP changes is addressed directly in terms of the classic ocean process called the oceanic inverted barometer. In the ideal case, SL rises (falls) 1.01 cm for each millibar of AP decrease (increase). That is in the ideal open ocean case AP/SL transfer coefficient, T_{ap-sl} , defined according to

$$T_{ap-sl} = \frac{R_{ap-sl}}{R_{ap-ap}},$$

where R_{ap-sl} is the cross-covariance between AP and SL and R_{ap-ap} is the auto-covariance of AP, is -1.01 cm/mb. Deep ocean observations (e.g. [Brown et al., 1975](#); [Wunsch and Stammer, 1997](#)) suggest that the deep ocean is very nearly a perfect inverted barometer (IB) to local AP fluctuations.

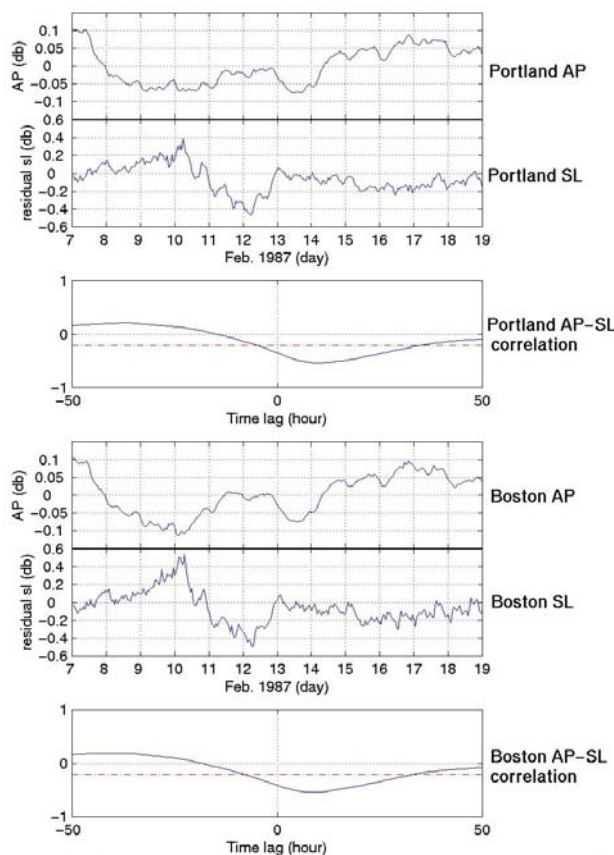


Figure A1. Portland and Boston atmospheric pressure (upper), residual sea level (middle) for 7-18 February 1987. The bottom panel shows correlation between air pressure and residual sea level for winter 1987.

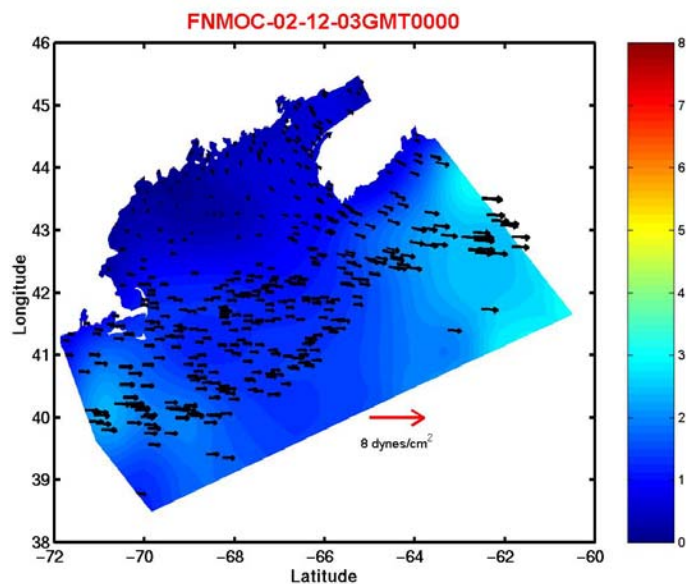
However, the ideal oceanic inverted barometer is not generally observed in the coastal ocean – primarily because of the effects of the coasts on the ocean response to propagating AP systems (see [Crepon, 1976](#) discussions) and the separate effects of wind stress forcing. So it is not surprising that the calculated local AP/SL transfer coefficients at both Portland and Boston ([Table A1](#)) are different than the classic IB *and different than each other*. These results suggest that 18% and 5% of the same AP fluctuation at Portland and Boston respectively could penetrate throughout the water column and thus could set up lateral pressure gradients that could be a factor in forcing a Gulf response.

Table A1. The atmospheric pressure (db)/sea level (db) transfer coefficients at Portland and Boston.

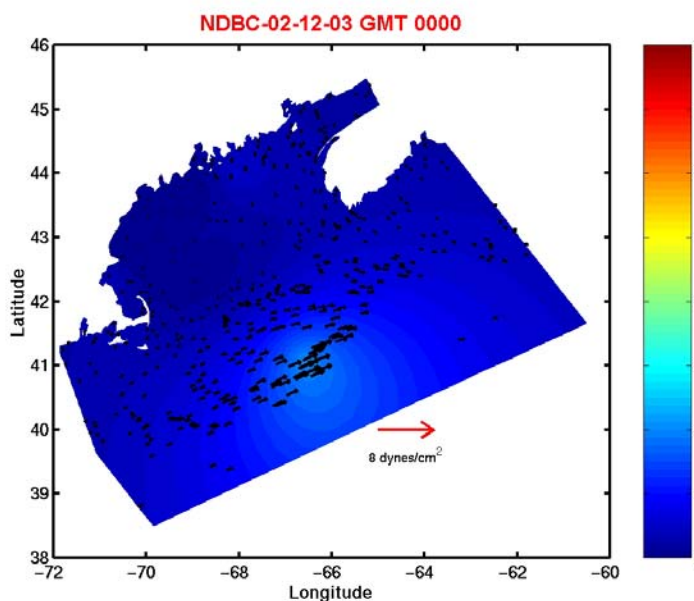
Station	R_{ap-sl} (db ²)	R_{ap-ap} (db ²)	T_{ap-sl} (db/db)
Portland	-0.0098	0.0119	-0.8235
Boston	-0.0109	0.0115	-0.9478

Appendix B. FNMOC versus NDBC-Derived Wind Stress

In this section we compare examples of the NDBC-derived wind stress fields for a February storm in 2003 (similar to our study) with wind stresses derived from U.S. Navy NO-GAPS (Navy Operational Global Atmospheric Prediction System used by FNMOC) winds. The strengths and weaknesses of the two representations are revealed in the examples we have chosen.



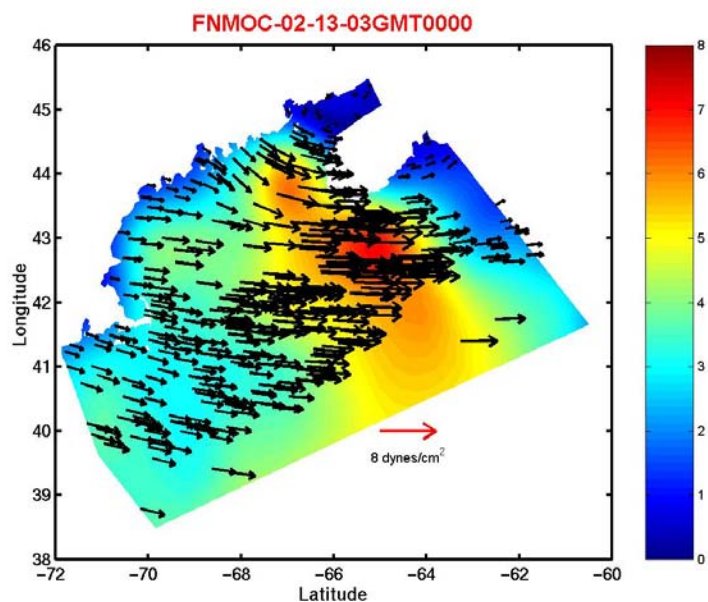
A



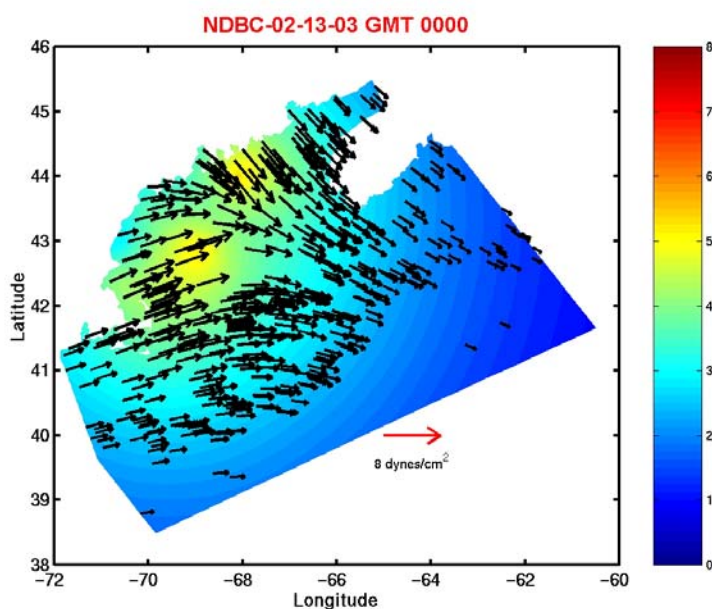
B

Figure B1. Wind stress fields based on (A) FNMOC and (B) NDBC winds at 0000 GMT 12 February 2003. The spatial-average wind stresses for FNMOC winds are 1.16 dyn/cm^2 ; and for NDBC 0.52 dyn/cm^2 . The magnitudes of the wind stresses are color-coded according to the legend on the right.

In the light wind stress case in [Figure B1](#) the fields are quite similar in the Gulf landward of Georges Bank. However the FNMOC wind stresses are larger on the seaward side. The real differences show up dramatically for the [Figure B2](#) case at the height of the storm, where the NDBC wind-stress field basically misses the strongest winds of the storm that are located in the eastern part of the model domain south of Nova Scotia. The third



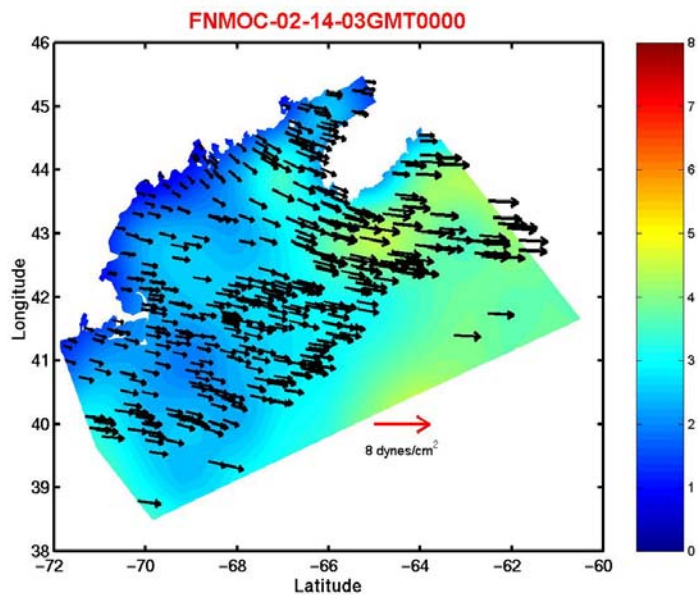
A



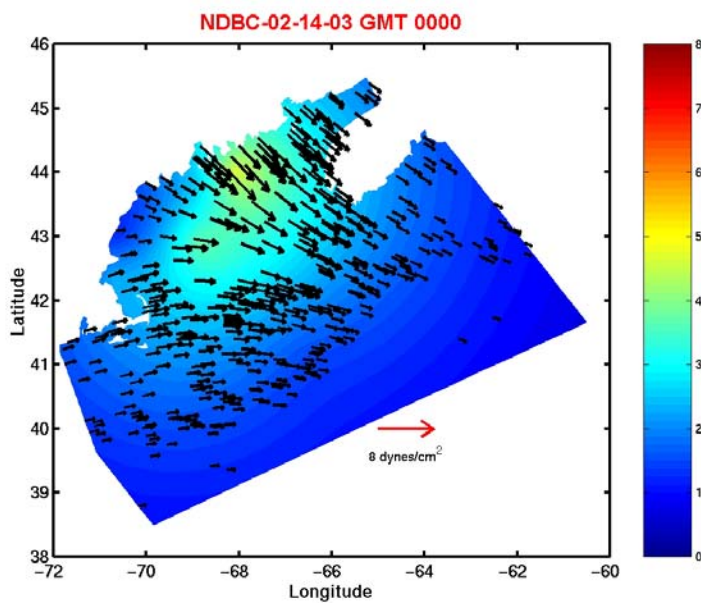
B

Figure B2. Wind stress fields based on (A) FNMOC and (B) NDBC winds at 0000 GMT 13 February 2003. The spatial-average wind stresses are 3.72 dyn/cm^2 for FNMOC and 3.07 dyn/cm^2 for NDBC. The magnitudes of the wind stresses are color-coded according to the legend on the right.

example in Figure B3 shows that on occasion how FNMOC can miss strong coastal Maine winds that NDBC is well-suited to detect. Thus neither approach is reliable all the time for specifying winds that are important to the gulf storm (and strong wind) response.



A



B

Figure B3. Wind stress fields based on (A) FNMOC and (B) NDBC winds at 0000 GMT 14 February 2003. The spatial-average wind stresses are 2.63 dyn /cm² for FNMOC and 2.18 dyn /cm² for NDBC. The magnitudes of the wind stresses are color-coded according to the legend on the right.

9. Acknowledgements

This research benefited greatly from the assistance provided by Chris Naimie who formerly resided in Daniel Lynch's Numerical Methods Laboratory in the Thayer School at Dartmouth College. The New Hampshire/Maine Sea Grant Program supported this work through grant R/CE-122.

10. References

- Blain, C.A., J.J. Westerink, and R.A. Luettich Jr., 1994. The influence of the domain size on the response characteristics of a hurricane surge model, *J. Geophys. Res.*, 99, 18,46 -18,479.
- Brown, W.S., W. Munk, F. Snodgrass, B. Zetler, and H. Mofjeld, MODE bottom experiment, *J. Phys. Oceanogr.*, 25,75-85.
- Brown, W.S., and J.D. Irish, 1992. The annual evolution of geostrophic flow in the Gulf of Maine: 1986-87, *J. Phys. Oceanogr.*, 22, 445-473.
- Brown, W.S., 1998. Wind-forced pressure response of the Gulf of Maine, *Journal of Geophysical Research*, 103 (C13), 30, 661-30,678.
- Brown, W. S., A. Gangopadhyay, F. L. Bub, Z. Yu and G. Strout, A. R. Robinson, 2004. An operational circulation modeling system for the Gulf of Maine /Georges Bank, Part1: Basic elements. (submitted to the *J. of Marine Systems*).
- Brown, W. S., A. Gangopadhyay, and Z. Yu, 2004. An operational circulation modeling system for the Gulf of Maine /Georges Bank, Part2: Applications. (submitted to the *J. of Marine Systems*).
- Csanady, G. T., 1978. The arrested topographic wave, *J. Phys. Oceanogr.*, 8, 47-62.
- Crepon, M. R., 1976. Sea level, bottom pressure and geostrophic adjustment, *Memoires Societe Royale des Sciences de Liege*, 6^e serie, tome X, 43-60.
- Fan, Y. and W. S. Brown, 2003. Simulations of the Gulf of Maine Storm Response Subject to Surface Wave-Induced Effects on Bottom Friction, *SMAST Technical Report No. 01-03-22*, pp 36. <http://www.smast.umassd.edu/OCEANOL/reports.php>
- Feng, H., and W.S. Brown, 1999. The wind-forced response of the western Gulf of Maine coastal ocean during spring and summer 1994, (unpublished manuscript).
- Flather, R.A., 1994. A storm surge prediction model for the northern Bay of Bengal with application to the cyclone disaster in April 1991, *J. Phys. Oceanogr.*, 24, 172-190.
- Holboke, Monica J., 1998. Variability of the Maine Coastal Current under Spring Conditions, Ph.D. Dissertation -Thayer School of Engineering -Dartmouth College, pp. 193.
- Large, W. G. and S. Pond, 1981. Open Ocean Momentum Flux Measurements in Moderately Strong Winds. *J. Phys. Oceanogr.*, 11, 639-657.
- Lynch, D. R., F. E. Werner, D. A. Greenberg, and J. W. Loder, 1992. Diagnostic Model for Baroclinic, Wind-driven and Tidal Circulation in Shallow Seas. *Continental Shelf Research*, Vol. 12, 37-64.
- Lynch, D. R., J. T. C. Ip, C. E. Naimie, and F. E. Werner, 1996. Comprehensive coastal circulation model with application to the Gulf of Maine, *Continental Shelf Research*, 16, 875-906.
- Lynch, D. R., M. J. Holboke, and C. E. Naimie, 1997. The Maine Coastal Current: Spring Climatological Circulation. *Continental Shelf Research*, 17, 605-634.
- Mupparapu, P. and W.S. Brown 2002. Role of convection in winter mixed layer formation in the Gulf of Main, February 1987. *Journal of Geophysical Research*, Vol. 107, No. C12, 3229
- Naimie, C. E., J. W. Loder, and D. R. Lynch, 1996. Seasonal variation of the three-dimensional residual circulation on Georges Bank. *Journal of Geophysical Research*, 101, 6469-6486.
- Styles, R. and S. M. Glenn, 2000. Modeling stratified wave and current bottom boundary layers on the continental shelf. *Journal of Geophysical Research*, 105, C10, 24119- ????
- Wunsch, C. and D. Stammer, 1997. Atmospheric loading and the oceanic "inverted barometer" effect, *Reviews in Geophysics*, 35, 1,79-107.
- Young B., Y. Lu, R. Greatbatch, 1995. Synoptic bottom pressure variability on the Labrador and Newfoundland Continental Shelves. *Journal of Geophysical Research*, 100, C5, 8639- 8653.